Hindawi
International Journal of Polymer Science
Volume 2018, Article ID 9783941, 6 pages
https://doi.org/10.1155/2018/9783941

Research Article

$CaCO_3$–Polymer Nanocomposite Prepared with Supercritical CO_2

Hiroaki Wakayama

Toyota Central R&D Laboratories, Inc., Nagakute, Aichi 480-1192, Japan

Correspondence should be addressed to Hiroaki Wakayama; wakayama@mosk.tytlabs.co.jp

Received 7 May 2018; Accepted 12 July 2018; Published 1 August 2018

Academic Editor: Yulin Deng

Copyright © 2018 Hiroaki Wakayama. This is an open access article distributed under the Creative Commons Attribution License, which permits unrestricted use, distribution, and reproduction in any medium, provided the original work is properly cited.

A novel process for generation of a $CaCO_3$–polymer nanocomposite with a controlled three-dimensional shape was developed. Specifically, a nanocomposite with a high $CaCO_3$ content was produced by introducing supercritical CO_2 into a polymer matrix containing Ca ions. A mixture of poly(vinyl alcohol), Ca acetate, and poly(acrylic acid) was poured into a mold, the mold was placed in an autoclave, and CO_2 was introduced to precipitate $CaCO_3$ within the polymer matrix. Laser Raman spectroscopy and transmission electron microscopy showed that this process produced a nanocomposite containing highly dispersed $CaCO_3$ (aragonite) nanoparticles. The flexural strength of the nanocomposite was larger than the flexural strengths of limestone and $CaCO_3$ produced by hydrothermal hot pressing. The use of supercritical CO_2 facilitated CO_2 dissolution, which resulted in rapid precipitation of $CaCO_3$ in the polymer matrix. The above-described process has potential utility for fixation of CO_2.

1. Introduction

The adverse environmental effects of human activities are becoming increasingly problematic. Minimizing energy consumption and waste generation during material production is therefore an important goal in the field of material engineering. One potential strategy for achieving this goal is to mimic processes and simulate materials found in living organisms.

Organisms synthesize inorganic substances such as hydroxyapatite, calcium carbonate ($CaCO_3$), and silica and organic substances such as cellulose and chitin at ambient temperature and atmospheric pressure [1]. These substances are eventually returned to the natural environment and are transformed into resources such as limestone and phosphate ores [2]. In addition, living organisms also serve as sources of materials, such as wood and tree lacquers, that can be used and reused by humans over the course of many centuries [3].

The highly controlled microstructures of living organisms are constructed from various molecular building blocks, and the organisms themselves can therefore be thought of as aggregates of sophisticated nanodevices [4]. By combining multiple types of organic molecules or by combining organic and inorganic molecules at the nanometer scale, organisms can carry out an astonishing array of functions that cannot be achieved with artificial devices.

Biomaterials represent a treasure trove of functional materials, and mimicking biological functions and effectively using biomaterials are major challenges in the field of materials engineering. Biomaterials such as bones, teeth, shells, and pearls are good models for the development of novel functional materials with minimal environmental loads and energy consumption. Designing and creating new functional materials based on substances, structures, functions, and processes of living things are called biomimetic materials processing, and functional materials generated by such processing are referred to as biomimetic functional materials [5]. One biological process that is of particular interest is biomineralization (i.e., biological synthesis of minerals). Because this process consumes little energy and emits little waste into the environment, it has an extremely low environmental burden. Therefore, imitation of biomineralization might lead to an environmentally friendly process for synthesis of ceramics.

Biominerals are not simple inorganic crystals but composites of inorganic and organic materials [6]. For example, shells consist of 95% $CaCO_3$ and 5% protein, a composition that imparts flexibility and structural anisotropy not found in pure $CaCO_3$ crystals. Several attempts to produce

composite materials by mimicking biomineralization have been reported [7–10]. However, in most cases, the $CaCO_3$ products obtained are powders with particle sizes of no more than a few micrometers. Although there have been a few reports of the formation of $CaCO_3$ thin films, the process takes several days [11]. More research is necessary for the development of versatile, industrially practical routes to bioinspired materials, such as the production of bulk $CaCO_3$ nanocomposite materials via rapid CO_2 fixation.

In this study, a novel process for producing $CaCO_3$ nanocomposite materials was developed. Specifically, glossy $CaCO_3$–polymer nanocomposites were produced by introducing supercritical CO_2 into aqueous Ca^{2+} in the presence of a polymer. In the work described in this paper, supercritical CO_2 was used to facilitate mineralization of $CaCO_3$ for production of a $CaCO_3$–polymer nanocomposite with a controlled three-dimensional shape. Specifically, a mixture of poly(vinyl alcohol) (PVA), Ca acetate, and poly(acrylic acid) (PAA) was poured into a mold, the mold was placed in an autoclave, and CO_2 was introduced to precipitate $CaCO_3$ within the polymer matrix. Laser Raman spectroscopy and transmission electron microscopy revealed that the resulting nanocomposite was composed of highly dispersed $CaCO_3$ (aragonite) nanoparticles and had excellent mechanical properties; its flexural strength was larger than the flexural strengths of limestone and $CaCO_3$ produced by hydrothermal hot pressing.

2. Experimental

2.1. Materials. PVA (100 g, $MW = 2 \times 10^3$) was dissolved in 500 mL of 1.42 M aqueous Ca acetate along with 2.4×10^{-3} wt% of PAA ($MW = 2 \times 10^3$). The mixture was stirred for 10 min, heated at 90°C for 3 h, and then poured into a mold. The mold was placed in an autoclave, CO_2 was introduced, and the autoclave was heated at 50°C and 10 MPa for 2 h. The sample was removed from the mold and cut into a rectangular parallelepiped in order to measure mechanical properties.

2.2. Analysis. X-ray diffraction patterns (Cu Kα) were collected on a diffractometer (RINT-TTR, Rigaku, Japan) operated at 40 kV and 50 mA. Scanning electron microscopy images and energy-dispersive X-ray spectra were obtained with a scanning electron microscope (S-3600N, Hitachi, Japan). Scanning transmission electron microscopy images were obtained with a transmission electron microscope (JEM-2010 FEF [HR], JEOL, Japan). Thermal decomposition of the samples up to 1273 K was measured with a thermogravimetric analysis instrument (Thermo Plus, Rigaku) under an air atmosphere. Raman spectra were recorded with a Raman spectrometer (NRS-3300, JASCO, Japan). Three-point bending tests were conducted with a testing machine (universal testing machine type 5966, Instron, USA).

3. Results and Discussion

A $CaCO_3$–polymer nanocomposite sample was prepared (Figure 1) via the procedure described in Section 2.1.

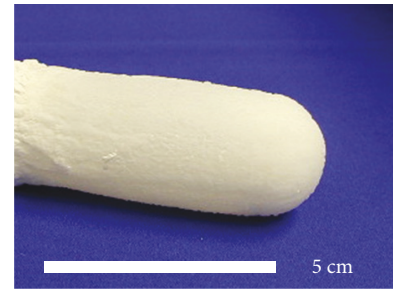

Figure 1: An external view of the $CaCO_3$–polymer nanocomposite sample.

The $CaCO_3$–polymer nanocomposite sample was subjected to thermogravimetric analysis (TGA) (Figure 2). The TGA trace revealed successive mass losses due to the removal of absorbed water and acetic acid, PVA degradation [12], and $CaCO_3$ decomposition [13] (Figure 2). The weight loss from 200 to 500°C was due to the dehydration reaction of –OH groups in the PVA chains and subsequent release of CO_2 gas due to degradation of PVA [12]. The amounts of CaO and ash produced were calculated from the weight loss of $CaCO_3$ (corresponding to the amount of CO_2 produced) when $CaCO_3$ decomposed into CaO and CO_2 at 600–700°C [13]. The attribution of the weight loss in each temperature range and the percentages of the total weight contributed by each component are shown in the TGA results (Figure 2). The overall percentage of $CaCO_3$ in the nanocomposite was estimated to be 57.3 wt%; that is, the $CaCO_3$ content was high. Producing nanocomposites containing large amounts of inorganic materials is difficult via conventional mixing processes [14].

The X-ray diffraction pattern of the nanocomposite sample showed only reflections corresponding to aragonite (Figure 3), which is less stable than calcite, the most stable $CaCO_3$ polymorph [15]. The production of aragonite was attributed to the templating effect of the hydroxyl groups of the PVA [16]. That is, the aragonite polymorph formed because the hydroxyl groups bonded to Ca^{2+} via PAA, and the arrangement of the hydroxyl groups was very similar to the arrangement of the atoms of aragonite. When PAA was adsorbed onto the crystalline form of PVA, a locally aligned two-dimensional structure formed in the PVA matrix. The templating effect of the PVA matrix resulted in the formation of aragonite crystals on this two-dimensional structure.

Electron micrographs of the $CaCO_3$–polymer nanocomposite sample were obtained (Figures 4(a) and 4(b)). The image shown in Figure 4(a) confirmed that ~3 μm $CaCO_3$ particles were embedded firmly in the polymer matrix. The columnar crystals that are characteristic of aragonite [17] were clearly observed in the magnified image shown in Figure 4(b). Surprisingly, calcium was detected at locations both on and near the particles. Specifically, in the energy-dispersive X-ray spectra, calcium was detected both in the smooth areas of the sample and in the areas with $CaCO_3$ particles (Figures 4(c) and 4(d)). This result suggested the formation of a nanocomposite structure consisting of fine $CaCO_3$ particles precipitated in a polymer matrix.

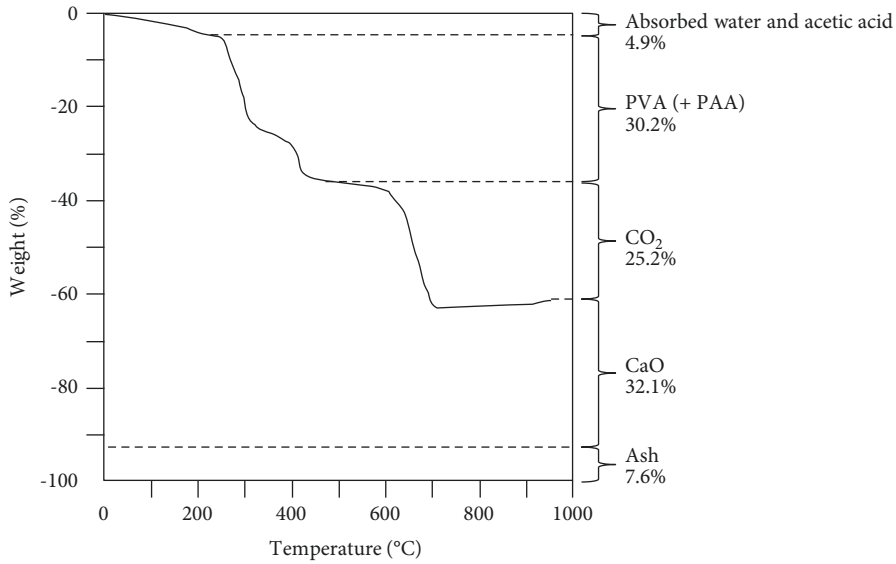

Figure 2: Thermal weight change of the $CaCO_3$–polymer nanocomposite sample.

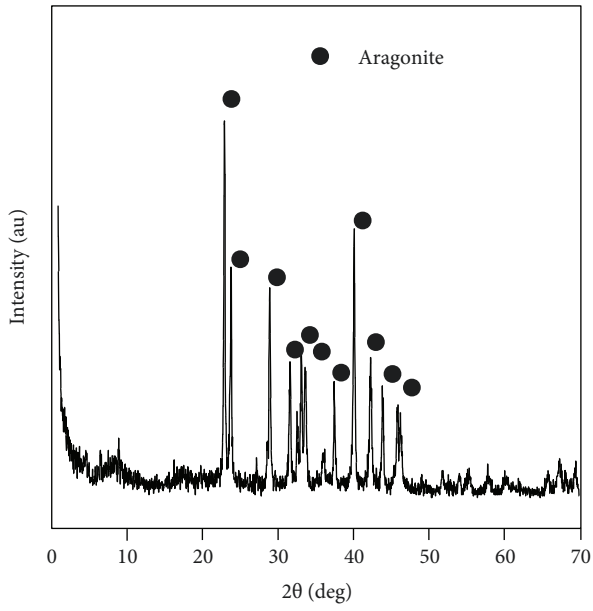

Figure 3: X-ray diffraction pattern of the $CaCO_3$–polymer nanocomposite sample.

Figure 5 shows the microscopic laser Raman spectrum of the $CaCO_3$–polymer nanocomposite sample. Peaks for $CaCO_3$ (aragonite) [18] were detected both in the parts of the sample corresponding to $CaCO_3$ particles and in the parts considered to consist mainly of PVA. This result suggested a nanocomposite structure of extremely fine $CaCO_3$ particles precipitated in the polymer matrix and was consistent with the energy-dispersive X-ray analysis result.

In the transmission electron microscopy image (Figure 6), the presence of fine particles (<10 nm) confirmed that the nanocomposite consisted of highly dispersed $CaCO_3$ nanoparticles in a polymer matrix. The image showed that $CaCO_3$ nanoparticles were dispersed in the PVA matrix (Figure 6). In contrast, as shown in the scanning electron microscopy images (Figures 4(a) and 4(b)), $CaCO_3$ microparticles with dimensions of several micrometers were also present in the samples. The TGA result showed that the content of $CaCO_3$ in the whole sample was relatively high. Even though $CaCO_3$ nanocomposites have previously been synthesized [14, 19, 20], synthesizing nanocomposites with a high $CaCO_3$ content remains challenging. For example, in a previous synthesis of $CaCO_3$ nanocomposites, $CaCO_3$ particles with dimensions of several tens of nanometers, synthesized in advance, were mixed with polymers, but when high concentrations of these $CaCO_3$ particles were mixed with the polymers, $CaCO_3$ aggregated [21]. In contrast, in this study, the use of supercritical CO_2 facilitated CO_2 dissolution, which resulted in rapid precipitation of $CaCO_3$ within the polymer matrix. That is, $CaCO_3$-containing nanoparticles with diameters of several nanometers formed in the polymer matrix, and these nanoparticles were finer than previously reported $CaCO_3$ nanoparticles. The functional groups in the polymer molecules probably acted as templates for the crystallization of $CaCO_3$ in the aragonite crystal structure, and even though the $CaCO_3$ content was high, $CaCO_3$ was highly dispersed in the polymer.

The flexural strength of the $CaCO_3$–polymer nanocomposite sample was 12 MPa, which is larger than the corresponding values for limestone and $CaCO_3$ produced by hydrothermal hot pressing (Figure 7). The strength of the nanocomposite was likely due to the existence of a nanocomposite structure in which $CaCO_3$ nanoparticles were more firmly attached to the polymer matrix than the particles in limestone or hot-pressed $CaCO_3$. Limestone and hot-pressed $CaCO_3$ consist of calcite, whereas the process reported herein produced aragonite, which is mechanically stronger than calcite [22].

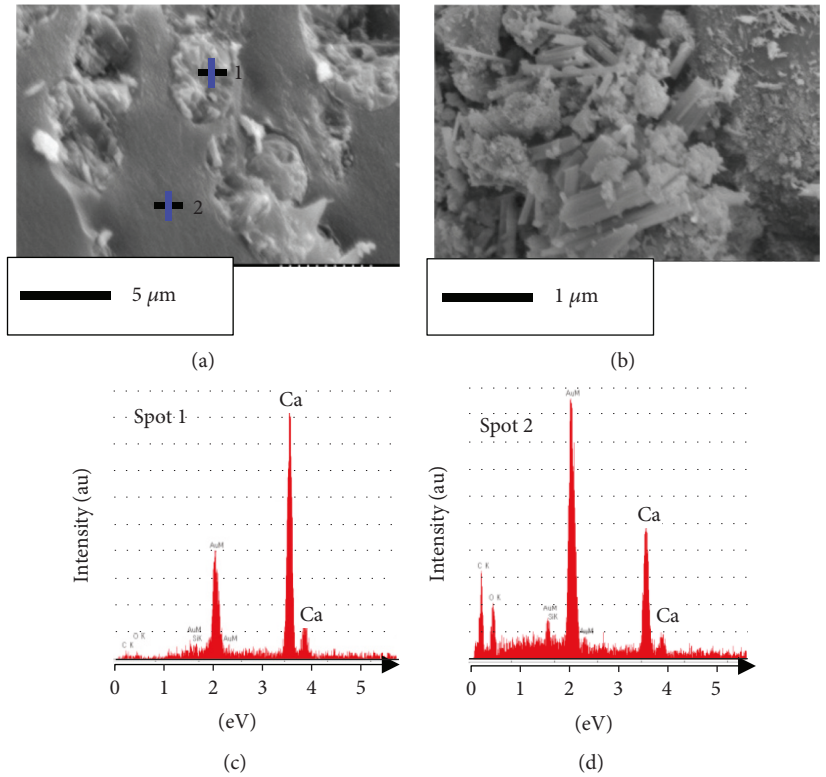

Figure 4: Scanning electron microscopy photographs of the $CaCO_3$–polymer nanocomposite sample (a and b) and corresponding energy-dispersive X-ray spectra (c and d).

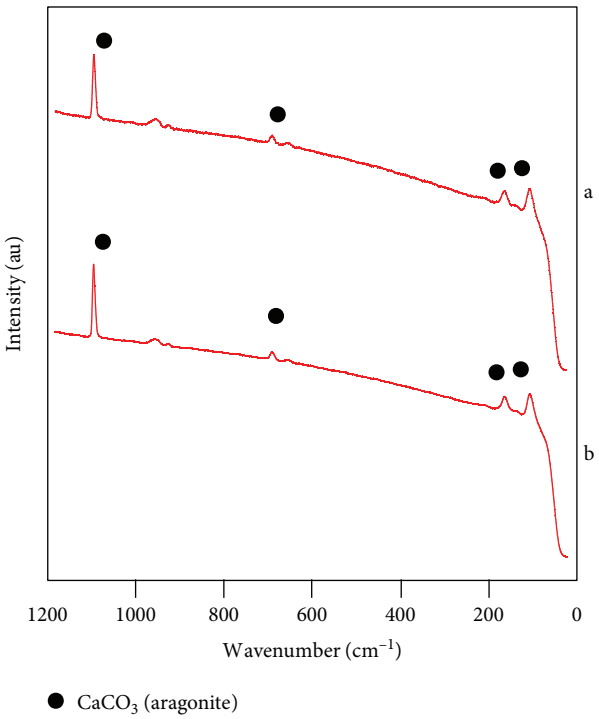

Figure 5: Laser Raman spectrum on (a) and near the $CaCO_3$ microparticle (b).

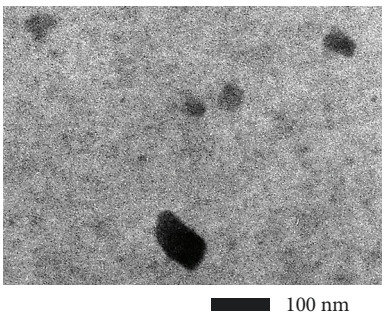

Figure 6: Transmission electron microscopy image of the $CaCO_3$–polymer nanocomposite sample.

4. Conclusion

A novel process for generation of a $CaCO_3$–polymer nanocomposite with a controlled three-dimensional shape was developed. The nanocomposite consisted of large amounts of $CaCO_3$ (aragonite) dispersed in a polymer matrix at the nanometer scale. The nanocomposite had excellent mechanical properties; its flexural strength was larger than the flexural strengths of limestone and $CaCO_3$ produced by hydrothermal hot pressing. The use of supercritical CO_2 facilitated CO_2 dissolution, which resulted in rapid precipitation of $CaCO_3$ in the polymer matrix. This process has potential utility for fixation of CO_2.

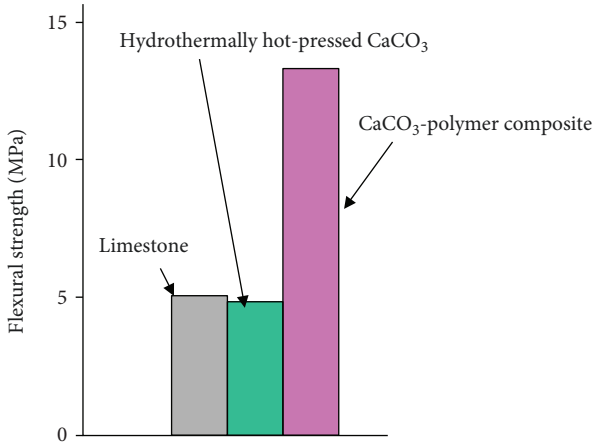

Figure 7: Flexural strength of the $CaCO_3$–polymer nanocomposite sample compared with strengths of limestone and $CaCO_3$ produced by hydrothermal hot pressing.

Data Availability

All the data used to support the findings of this study are available from the corresponding author upon request.

Disclosure

The research was performed as part of the author's job with the Toyota Central R&D Labs. Inc.

Conflicts of Interest

The author declares no conflicts of interest.

References

[1] R. Sahay, P. S. Kumar, R. Sridhar et al., "Electrospun composite nanofibers and their multifaceted applications," *Journal of Materials Chemistry*, vol. 22, no. 26, pp. 12953–12971, 2012.

[2] Y. Xu, C. Luo, Y. Zheng, H. Ding, D. Zhou, and L. Zhang, "Natural calcium-based sorbents doped with sea salt for cyclic CO_2 capture," *Chemical Engineering & Technology*, vol. 40, no. 3, pp. 522–528, 2017.

[3] K. Yuasa, T. Honda, R. Lu, T. Hachiya, and T. Miyakoshi, "Analysis of Japanese ancient lacquerwares excavated from Jōmon period ruins," *Journal of Analytical and Applied Pyrolysis*, vol. 113, pp. 73–77, 2015.

[4] A. Bertucci, J. Guo, N. Oppmann et al., "Probing transcription factor binding activity and downstream gene silencing in living cells with a DNA nanoswitch," *Nanoscale*, vol. 10, no. 4, pp. 2034–2044, 2018.

[5] X. Zhang, M. Lu, Y. Wang, X. Su, and X. Zhang, "The development of biomimetic spherical hydroxyapatite/polyamide 66 biocomposites as bone repair materials," *International Journal of Polymer Science*, vol. 2014, Article ID 579252, 6 pages, 2014.

[6] T. Chen, P. Shi, Y. Li et al., "Biomineralization of varied calcium carbonate crystals by the synergistic effect of silk fibroin/magnesium ions in a microbial system," *CrystEngComm*, vol. 20, no. 17, pp. 2366–2373, 2018.

[7] J. X. Hu, J. B. Ran, S. Chen, X. Y. Shen, and H. Tong, "Biomineralization-inspired synthesis of chitosan/hydroxyapatite biocomposites based on a novel bilayer rate-controlling model," *Colloids and Surfaces B: Biointerfaces*, vol. 136, pp. 457–464, 2015.

[8] Z. Li, G. Zhou, H. Dai et al., "Biomineralization-mimetic preparation of hybrid membranes with ultra-high loading of pristine metal–organic frameworks grown on silk nanofibers for hazard collection in water," *Journal of Materials Chemistry A*, vol. 6, no. 8, pp. 3402–3413, 2018.

[9] J. C. Munyemana, H. He, S. Ding, J. Yin, P. Xi, and J. Xiao, "Synthesis of manganese phosphate hybrid nanoflowers by collagen-templated biomineralization," *RSC Advances*, vol. 8, no. 5, pp. 2708–2713, 2018.

[10] F. Leroux, P. Rabu, N. A. J. M. Sommerdijk, and A. Taubert, "Hybrid materials engineering in biology, chemistry, and physics," *European Journal of Inorganic Chemistry*, vol. 2015, no. 7, pp. 1086–1088, 2015.

[11] S. Matsumura, S. Kajiyama, T. Nishimura, and T. Kato, "Formation of helically structured chitin/$CaCO_3$ hybrids through an approach inspired by the biomineralization processes of crustacean cuticles," *Small*, vol. 11, no. 38, pp. 5127–5133, 2015.

[12] S. Kayal and R. V. Ramanujan, "Doxorubicin loaded PVA coated iron oxide nanoparticles for targeted drug delivery," *Materials Science and Engineering: C*, vol. 30, no. 3, pp. 484–490, 2010.

[13] S. Sun, D. Gebauer, and H. Colfen, "A solvothermal method for synthesizing monolayer protected amorphous calcium carbonate clusters," *Chemical Communications*, vol. 52, no. 43, pp. 7036–7038, 2016.

[14] X. Gao, C. Deng, C. Ren, J. Zhang, Z. Li, and K. Shen, "Mechanical properties and morphology of polypropylene-calcium carbonate nanocomposites prepared by dynamic packing injection molding," *Journal of Applied Polymer Science*, vol. 124, no. 2, pp. 1392–1397, 2012.

[15] M. E. Arroyo-de Dompablo, M. A. Fernández-González, and L. Fernández-Díaz, "Computational investigation of the influence of tetrahedral oxoanions (sulphate, selenate and chromate) on the stability of calcium carbonate polymorphs," *RSC Advances*, vol. 5, no. 74, pp. 59845–59852, 2015.

[16] L. Xu, X. Zhao, C. Xu, and N. A. Kotov, "Water-rich biomimetic composites with abiotic self-organizing nanofiber network," *Advanced Materials*, vol. 30, no. 1, article 1703343, 2018.

[17] J. Küther, R. Seshadri, W. Knoll, and W. Tremel, "Templated growth of calcite, vaterite and aragonite crystals onself-assembled monolayers of substituted alkylthiols on gold," *Journal of Materials Chemistry*, vol. 8, no. 3, pp. 641–650, 1998.

[18] M. De La Pierre, C. Carteret, L. Maschio, E. André, R. Orlando, and R. Dovesi, "The Raman spectrum of $CaCO_3$ polymorphs calcite and aragonite: a combined experimental and computational study," *The Journal of Chemical Physics*, vol. 140, no. 16, article 164509, 2014.

[19] A. Elloumi, S. Pimbert, and C. Bradai, "Phase structure and mechanical properties of PP/EPR/$CaCO_3$ nanocomposites: effect of particle's size and treatment," *Polymer Engineering and Science*, vol. 55, no. 12, pp. 2859–2868, 2015.

[20] W. Gao, L. Ding, and Y. Zhu, "Effect of surface modification on the dispersion, thermal stability and crystallization

properties of PET/$CaCO_3$ Nanocomposites," *Tenside Surfactants Detergents*, vol. 54, no. 3, pp. 230–237, 2017.

[21] L. Jiang, J. Zhang, and M. P. Wolcott, "Comparison of polylactide/nano-sized calcium carbonate and polylactide/montmorillonite composites: reinforcing effects and toughening mechanisms," *Polymer*, vol. 48, no. 26, pp. 7632–7644, 2007.

[22] A. D. Chervonnyi, "Effect of $CaCO_3$ polymorphs on the strength of a calcium aluminosilicate composite," *Inorganic Materials*, vol. 39, no. 4, pp. 386–391, 2003.


The Scientific
World Journal
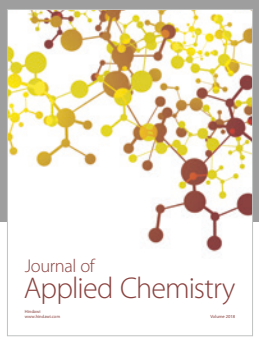
Journal of
Applied Chemistry
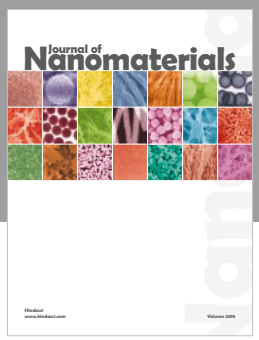
Journal of
Nanomaterials

Scientifica

International Journal of
Polymer Science
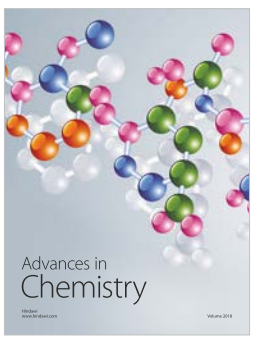
Advances in
Chemistry

Hindawi
Submit your manuscripts at
www.hindawi.com
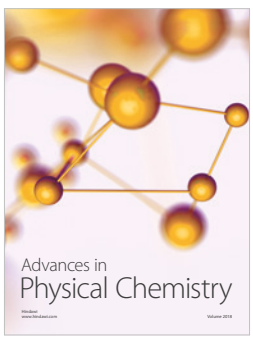
Advances in
Physical Chemistry

International Journal of
Analytical Chemistry
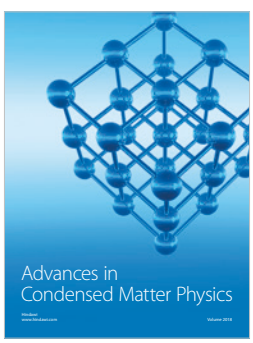
Advances in
Condensed Matter Physics
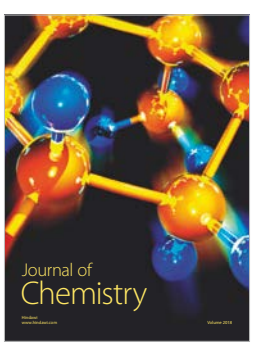
Journal of
Chemistry

International Journal of
Biomaterials
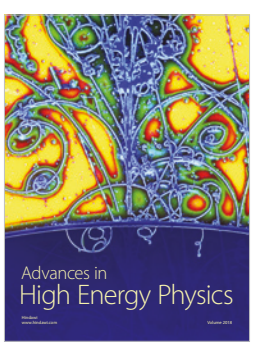
Advances in
High Energy Physics

Journal of
Engineering

Journal of
Nanotechnology

International Journal of
Corrosion

Journal of
Materials

BioMed
Research International
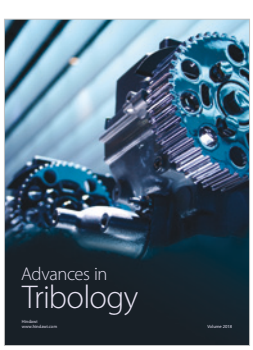
Advances in
Tribology
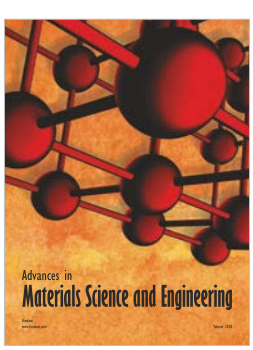
Advances in
Materials Science and Engineering